Thermodynamic Properties of Aqueous Dextran Solutions from Laser-Light-Scattering, Membrane Osmometry, and Isopiestic Measurements

H.-P. Kany,[†] H. Hasse,[‡] and G. Maurer*

Lehrstuhl für Technische Thermodynamik, Universität Kaiserslautern, Postfach 3049, 67653 Kaiserslautern, Germany

The thermodynamic properties of dextran (DEX) in aqueous solutions were studied by light-scattering, membrane osmometry, and isopiestic measurements. Five polymer samples of weight-average molecular mass between about 40 000 and 500 000 were investigated at temperatures between 293 K and 303 K. The experimental results are described with application of the osmotic virial equation. It was found that the new experimental data, as well as the literature data, can be described using second and third virial coefficients which do not depend on the molecular mass of the dextran.

Introduction

Natural dextran polymers (DEX) play an important role in medicine, in the pharmaceutical industry, and in biotechnology. Despite their importance, only very few thermodynamic data for these polymers in aqueous solutions are available. The present work reports on experimental investigations of aqueous dextran solutions by multiangle laser-light-scattering photometry, membrane osmometry, and isopiestic measurements. The experimental results are evaluated to determine second and third osmotic virial coefficients following a recently published procedure (Hasse et al., 1995). This procedure is based on the simultaneous evaluation of experimental data for dilute and concentrated aqueous solutions. It offers essential advantages over the common procedure in which data sets taken from different experimental methods are separately evaluated. Previously, that procedure was only applied to narrowly distributed poly(ethylene glycol). In the present paper, it is extended to polydisperse dextran. Figure 1 shows the structural formula of DEX.

Thermodynamic properties of DEX in aqueous solutions (DEX(aq)) have been studied by several authors. A comprehensive survey of the literature data is given in Table 1. There are large discrepancies in that literature data. One example is shown in Figure 2, where data for the second osmotic virial coefficient of DEX(aq) at ambient temperature are given. Discrepancies of up to 50% are observed. One reason for such discrepancies might result from neglect of the polydispersity of dextran. Second osmotic virial coefficients were reduced from experimental data, assuming that the aqueous DEX solution is a binary system; thus, the broad molecular mass distribution of DEX was neglected. To avoid uncertainties resulting from such an assumption, in the present work the osmotic virial equation was expanded by taking the polydispersity of the polymer into consideration. Another reason for the large discrep-
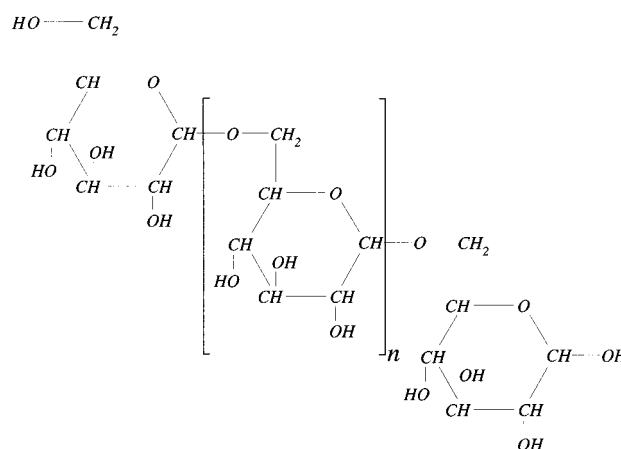

Figure 1. Structural formula of dextran.

ancies in literature data on the second osmotic virial coefficient might be that, in evaluating experimental data, contributions from the third osmotic virial coefficient are generally neglected. This may result in wrong values for the second virial coefficient (Hasse et al., 1995).

In the present work, thermodynamic properties of aqueous solutions of dextran were determined with three different methods: laser-light-scattering, membrane osmometry, and isopiestic measurements. The results were simultaneously evaluated using the expanded osmotic virial equation to determine the second and third osmotic virial coefficients of DEX(aq) at temperatures between 293 K and 303 K.

Experimental Section

Materials. In the present work aqueous solutions of five different dextran samples, designated here as DEX 40S, DEX 40VC, DEX 70S, DEX 110S, and DEX 500, were studied. DEX 40S, 70S, and 110S were supplied by Pfeiffer & Langen Organica, Dormagen, Germany (lot numbers 40861800, 1.0003.1.02, and 1108704). DEX 40VC was purchased from Serva GmbH, Heidelberg, Germany (lot number 21072) and DEX 500 from Pharmacia LKB Biotechnology AB, Uppsala, Sweden (lot number RK14758).

* To whom all correspondence should be addressed.
† Present address: Aventis Research & Technologies, GmbH & Co. KG, D-65926 Frankfurt, Germany.
‡ Present address: Institut für Technische Thermodynamik und Thermische Verfahrenstechnik, Universität Stuttgart, D-70550 Suttgart, Germany.

Table 1. Survey of Experimental Data on Thermodynamic Properties of Aqueous DEX Solutions

method	DEX	T/K	source[a]
differential vapor pressure	70, 500	298	Haynes et al., 1989*
vapor-pressure osmometry	40, 70, 110, 500	293, 313, 333	Gaube et al., 1993*
	0.6–9[b]	311, 333	Gekko, 1971; Gekko and Noguchi, 1971
membrane osmometry	40, 70, 150, 500	295	Edsman and Sundelöf, 1988
	40, 70, 110, 500	293, 313, 333	Gaube et al., 1993*
	500, 2000	na	Granger et al., 1985
	10	297	Jonsson, 1984*
	130, 190, 250	298	Mariani et al., 1955*
	10	298	Pusch, 1988
	70, 150, 250, 500, 2000	298	Smit et al., 1992
	40, 500	298	Vink, 1971*
light scattering	40, 80, 150, 250, 500, 2000	293	Burchard and Pfannenmüller, 1969
	158	280, 292, 306	Comper and Laurent, 1978*
	22–723[c]	293	Granath, 1958
	176–21 700[d]	298, 313, 328, 343	Jeremić et al., 1992
	70, 500	298	King et al., 1988
	80–100 000[e]	288, 298, 313, 323, 333	Nordmeier, 1993a,b
	10, 40	298	Rathbone et al., 1990
	18–9500[f]	298	Senti et al., 1955
	40, 70, 110, 500	293	Stumpf, 1993*
isopiestic method	500	293, 333	Grossmann et al., 1995[g]
sedimentation	27, 37, 51, 78	301	Edmond and Ogston, 1968
	22–723[d]	293	Granath, 1958
	18–9500[f]	298	Senti et al., 1955
calorimetry	1, 10, 1200	298	Basedow et al., 1980
	158	298	Comper and Laurent, 1978
	500	298, 333	Grossmann et al., 1995*

[a] Asterisks indicate sources in which numerical primary data are reported. [b] Six molecular weights between about 600 and 9000. [c] Nine molecular weights between about 2.1×10^4 and 7.2×10^5. [d] Twelve molecular weights between about 1.7×10^5 and 2.1×10^7. [e] Seven molecular weights between about 8×10^4 and 1×10^8. [f] Twenty-four molecular weights between about 1.8×10^4 and 9.5×10^6. [g] Included in the evaluation of the present work.
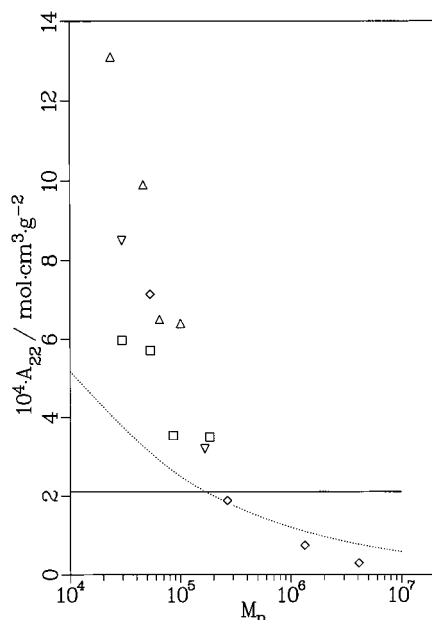

Figure 2. Second osmotic virial coefficients A_{22} of DEX in aqueous solution at about 298 K. Literature data obtained with different methods (cf. Table 1): ◇, Nordmeier (1993); △, Gaube et al. (1993); ▽, Haynes et al. (1989); □, Edsman and Sundelöf (1988); —, this work assuming $A_{22} = f(M_{DEX})$; - -, this work assuming $A_{22} \neq f(M_{DEX})$.

Figure 3. Differential molecular weight distributions of dextran determined by GPC: − - −, DEX 40S; −·−, DEX 40VC; - -, DEX 70S; ···, DEX 110S; —, DEX 500.

HPLC water (Merck, Darmstadt, Germany; impurities below 5 mg/kg) was used for the preparation of all solutions.

All dextrans were dissolved in water and characterized by gel permeation chromatography (GPC). These measurements were carried out with a GPC system (three columns filled with HEMA gel, porosity 40, 100, and 1000 Å; PSS, Mainz, Germany) c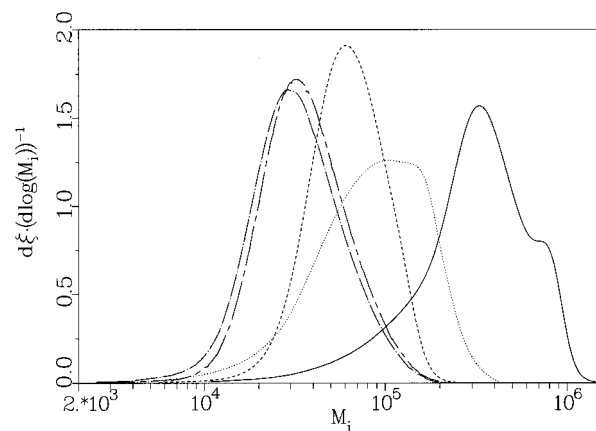oupled with a multiangle laser-light-scattering photometer (Wyatt Technology, Santa Barbara, CA; type DAWN F) and an interferometric refractometer (Wyatt; type Optilab 903). Details of the experimental arrangement and procedure are similar to those applied by Jackson et al. (1989) and have been described before (Hasse et al., 1995). The experimental results for the differential molecular weight distribution are shown in Figure 3. From these distributions the number-average molecular weight

$$M_n = \frac{\sum_{\text{all fractions } i} n_i M_i}{\sum_{\text{all fractions } i} n_i} \quad (1)$$

and the weight-average molecular weight

$$M_w = \frac{\sum\limits_{\text{all fractions } i} w_i M_i}{\sum\limits_{\text{all fractions } i} w_i} \qquad (2)$$

were calculated.

The numbers of M_n and M_w for all dextrans are compared with suppliers' data and results from simultaneous evaluation of laser-light-scattering data, osmometric data, and isopiestic data in Table 2 (for a discussion, see below).

Densimetric Data. For the conversion of polymer mass fractions $\xi_i = m_i/(m_1 + m_i)$ into concentrations $c_i = m_i/V$, the specific density $\rho^* = (m_1 + m_i)/V$ of the aqueous dextran solution has to be known:

$$c_i = \rho^* \xi_i \qquad (3)$$

Several authors have measured the specific density of aqueous dextran solutions (Albertson, 1986; Cesi et al., 1994; Johansson and Joelsson, 1992) up to about 0.2 g cm^{-3} at temperatures around 293 K. In the present work, the temperature and concentration ranges were extended (T/K = 293 and 313 and ρ^*/(g cm^{-3}) $\leq$ 0.35). The results are given in Appendix A.

Laser-Light Scattering. For each polymer, a stock solution of about 80 g containing between about 0.2 and 1.0 mass % dextran was prepared using an analytical balance with a resolution of 0.1 mg (Mettler, Giessen, Germany; type AE 240). Solutions of dextran are known to contain molecular aggregates (Fedin et al., 1975). To dissolve these aggregates, the stock solutions were treated in a water bath at 80 °C for about 30 min (Gaube et al., 1993). The aggregates can be determined by multiangle laser-light scattering (MALLS): the determined (apparent) molecular mass increases with an increasing degree of aggregation. No reaggregation was observed when the solutions were stored at ambient temperature. For each polymer, six samples were prepared by diluting the stock solutions. The concentration range of the laser-light-scattering experiments depends on the molecular mass of dextran. For example, in the aqueous solutions of DEX 40S the dextran concentrations were between 1.8×10^{-3} and 1.2×10^{-2} g cm^{-3}, whereas the dextran concentrations were 1 order of magnitude smaller in aqueous solutions of DEX 500.

All measurements were carried out at 293.15 K. For the evaluation of laser-light-scattering data, the optical constant K and the refractive index increment $(\partial n/\partial c_s)$ are required. The optical constant K is

$$K = \frac{4\pi^4 n_1^2 (\partial n/\partial c_s)^2}{N_A \lambda^4} \qquad (4)$$

where n_1 is the refractive index of the pure solvent, which was taken from Riddick et al. (1986). N_A is Avogadro's number, and λ is the laser wavelength (λ = 633 nm). The increment $(\partial n/\partial c_s)$ was determined using a interferometric refractometer (see above) at λ = 633 nm. (For a detailed description of the refractometer and the experimental procedure, see Hasse et al. (1995)). In the ranges studied ($0.5 \times 10^{-3} \leq c_s$/(g cm^{-3}) $\leq 4.0 \times 10^{-3}$ and 40 000 $\leq M_w$/(g mol^{-1}) $\leq$ 500 000) the experimental result for the refractive index increment depends neither on the molecular mass of dextran nor on the concentration: $\partial n/\partial c_s$/(cm^3 g^{-1}) = 0.147. That value is in good agreement with literature data (from Jackson et al. (1989), 0.145 cm^3 g^{-1}; from Williams

et al. (1992)), 0.146 cm^3 g^{-1}; from Nordmeier, (1993a), 0.148 cm^3 g^{-1}; from Rathbone et al. (1990)), (DEX 40) 0.151 cm^3 g^{-1} and (DEX 70 and DEX 500) 0.147 cm^3 g^{-1}, etc.).

The results of the laser-light-scattering experiments were given by Kany (1998).

Membrane Osmometry. For the measurement of the osmotic pressure of aqueous DEX solutions, a membrane osmometer (Gonotec, Berlin, Germany; type Osmomat 090) was used. The osmometer was equipped with semipermeable membranes (Filtron, Karlstein, Germany; type Omega) with an exclusion size of about 1000 g mol^{-1}. The osmometer was calibrated by applying hydrostatic pressures. The measurements were carried out against pure water at (303.15 $\pm$ 1) K. Four to six samples of each aqueous DEX solution were prepared in the same manner as described above. The concentration of DEX ranged from about 1.8×10^{-2} to 5.1×10^{-2} g cm^{-3} for DEX 40S and from about 2.5×10^{-2} to 6.6×10^{-2} g cm^{-3} for DEX 500. About 2 to 5 min after injection of the solution, the signal of the membrane osmometer was stable; i.e., equilibrium was reached. Because of the low exclusion size of the membrane, permeation of dextran molecules through the membrane is neglected. For each dextran and concentration, between three and five measurements were made. The results could be reproduced within the estimated accuracy of about $\pm$5%. The experimental results are given in Table 7 of Appendix B.

Isopiestic Method. The apparatus and the experimental procedure used for the isopiestic investigations have been described before (Grossmann et al., 1995). The isopiestic data on DEX 500 were taken from that publication (ξ_s/(g g^{-1}) $\approx$ 0.20−0.55, corresponding to c_s/(g cm^{-3}) $\approx$ 0.21−0.70). The activity of water in aqueous solutions of DEX 40S, 40VC, 70S, and 110S was measured at 293.15 K at polymer mass fractions between about 34% and 46% (corresponding to c_s/(g cm^{-3}) $\approx$ 0.35−0.55). The results are given in Table 8 of Appendix C. The maximum uncertainties of these data are estimated to $\pm$0.1 K in the temperature, $\pm$0.002 g g^{-1} in the polymer concentration, and $\pm$0.001 in the activity of water.

Correlation

Model. The osmotic virial equation is used to describe the thermodynamic properties of aqueous solutions of dextran. It is common practice to assume that also solutions of polydisperse polymers can be described with this equation; i.e., the influence of polydispersity of the polymer is usually neglected (e.g., see Rathbone et al. (1990)), Gaube et al. (1993), and King et al. (1988)). This assumption is invalid if the virial coefficients depend on the polymer molecular mass. In that case, the polydispersity has to be explicitly taken into account in the osmotic virial equation. The polydispersity of the polymer can be described either by a polymer mass distribution or by splitting the polydisperse polymer in a certain number of "monodisperse" pseudocomponents. The latter method is easier to handle and proved to be sufficient for the purpose of the present work. Thus, it is assumed that the polydisperse polymer consists of ($i = 2, ..., N$), i.e., $N - 1$ monodisperse polymers. The distribution is characterized by the mass fraction ξ_i of each (monodisperse) polymer i in the polydisperse polymer sample. The osmotic virial equation is based on a Taylor series expansion of the activity coefficients of the solutes, ln γ_i, in concentration c_i, i.e., mass of polymer per volume, around the ideal solution (ln $\gamma_i = 0$ at $c_i = 0$ in pure solvent), where the chemical potential μ_i of the solute (i) is normalized according to Henry's law ($c_i \rightarrow 0$ for interactions

Table 2. Experimental Data on the Number- and Weight-Average Molecular Weights of the Dextran Used in the Present Work

| | M_w | | | | M_n | | | | M_w/M_n MALLS, MO, ISO |
| | GPC | | MALLS, MO, ISO | | GPC | | MALLS, MO, ISO | | |
	supplier	this work	method I	method II	supplier	this work	method I	method II	method II
DEX 40S	40 350	41 370	35 853	33 946	25 881	31 564	28 191	26 192	1.30
DEX 40VC	39 081	38 205	34 790	32 300	27 080	28 263	26 112	24 029	1.34
DEX 70S	66 668	67 996	61 388	60 113	41 409	55 689	38 922	36 882	1.63
DEX 110S	108 198	102 296	103 732	103 577	56 946	63 955	56 888	54 526	1.90
DEX 500	502 000	481 000	438 954	448 327	182 000	223 000	132 236	169 337	2.65

and $c_i \rightarrow 1$ g cm^{-3} for concentration, both in pure solvent):

$$\ln \gamma_i = \sum_{j=2}^{N} \frac{\partial \ln \gamma_i}{\partial c_j}\bigg|_{\text{pure solvent}} c_j +$$

$$\frac{1}{2}\sum_{j=2}^{N}\sum_{k=2}^{N} \frac{\partial^2 \ln \gamma_i}{\partial c_j \, \partial c_k}\bigg|_{\text{pure solvent}} c_j c_k + \dots \quad (5)$$

Introducing abbreviations for partial derivatives similar to those for a binary system

$$a_{ij} = \frac{\partial \ln \gamma_i}{\partial c_j}\bigg|_{\text{pure solvent}} \quad (6)$$

$$a_{ijk} = \frac{\partial^2 \ln \gamma_i}{\partial c_j \, \partial c_k}\bigg|_{\text{pure solvent}} \quad (7)$$

leads to

$$\ln \gamma_i = \sum_{j=2}^{N} a_{ij} c_j + \frac{1}{2}\sum_{j=2}^{N}\sum_{k=2}^{N} a_{ijk} c_j c_k \quad (8)$$

The activity of the solvent follows from an integration of the Gibbs−Duhem equation, taking into account the symmetry of the virial coefficients as well as assuming $\rho_{\text{solution}} \approx \rho_{\text{pure solvent}}$ (for a detailed derivation, see, e.g., Kurata (1982)):

$$\ln a_1 = -\frac{c_s}{\rho_1}\left(\frac{1}{M_n} + A_2^{\text{osm}} c_s + A_3^{\text{osm}} c_s^2 + \dots\right) \quad (9)$$

where

$$A^{\text{osm}}_2 = \sum_{i=2}^{N}\sum_{j=2}^{N} \xi_i \xi_j A_{ij} \quad (10)$$

$$A^{\text{osm}}_3 = \sum_{i=2}^{N}\sum_{j=2}^{N}\sum_{k=2}^{N} \xi_i \xi_j \xi_k A_{ijk} \quad (11)$$

$$c_s = \sum_{i=2}^{N} c_i \quad (12)$$

A_2^{osm} and A_3^{osm} are the second and third osmotic virial coefficients of the polydisperse polymer in the solvent, respectively. The mixed virial coefficients A_{ij} and A_{ijk} ($i \neq j \neq k$) are directly related to the partial derivatives in eqs 6 and 7:

$$A_{ij} = \frac{a_{ij}}{2M_{n,i}} \quad (13)$$

$$A_{ijk} = \frac{a_{ijk}}{3M_{n,i}} \quad (14)$$

Table 3. Parameters of the Particle Scattering Function P_θ (Equation 18)

	method I	method II
$\Lambda_{1,\text{DEX40S}}$	0.29	0.41
$\Lambda_{1,\text{DEX40VC}}$	0.28	0.46
$\Lambda_{1,\text{DEX70S}}$	0.24	0.30
$\Lambda_{1,\text{DEX110S}}$	0.28	0.33
$\Lambda_{1,\text{DEX500}}$	0.09	0.14

c_s is the total concentration of the polymer, M_n is the number-average molecular mass of the polydisperse polymer, and ξ_i is the mass fraction of (monodisperse) component i of the polydisperse polymer.

A similar derivation with fixed temperature and fixed chemical potential μ_1 of the solvent (instead of a fixed or neglected pressure) leads to the expression for the osmotic pressure π^* of a solution of a polydisperse polymer (cf. Kurata (1982)):

$$\frac{\pi^*}{RT} = c_s\left(\frac{1}{M_n} + A_2^{\text{osm}} c_s + A_3^{\text{osm}} c_s^2 + \dots\right) \quad (15)$$

where the virial coefficients A_2^{osm} and A_3^{osm} are also given by eqs 10−14.

The basic equation for the evaluation of laser-light-scattering data in multicomponent systems has been developed independently by Kirkwood and Goldberg (1950) and by Stockmayer (1949). Using the osmotic virial equation, i.e., eq 9, for a system of a polydisperse polymer in a single solvent at constant pressure and temperature and assuming that the refractive index increment does not depend on the molecular mass of the polymer results in (cf. Kurata (1982))

$$\frac{Kc_s}{R_\theta^E} = \frac{1}{M_w P_\theta} + 2A_2^{\text{LS}} c_s + 3A_3^{\text{LS}} c_s^2 + \dots \quad (16)$$

K is the optical constant given by eq 4, and R_θ^E is the excess Rayleigh ratio. The excess Rayleigh ratio accounts primarily for the difference between the intensity of light scattered from the polymer solution to that scattered from the pure solvent. M_w is the weight-average molecular mass of the polymer. The particle scattering function P_θ has been introduced to describe the angular dependence of the Rayleigh ratio. P_θ is defined as the ratio of the excess Rayleigh ratios at the angle of observation θ, i.e., R_θ^E, and at $\theta = 0$, i.e., $R_{\theta,0}^E$, (cf. Kratochvíl (1987)):

$$P_\theta = R_\theta^E/R_{\theta,0}^E \quad (17)$$

P_θ (Table 3) was approximated by (cf. Appendix D)

$$P_\theta = 1 + \Lambda_1 \sin^4(\theta/2) \quad (18)$$

Λ_1 is considered to be an adjustable parameter characterizing each polydisperse polymer sample (i.e., $\Lambda_{1,\text{DEX40S}} \neq \Lambda_{1,\text{DEX40VC}} \neq \dots$).

A_2^{LS} and A_3^{LS} are the light-scattering second and third virial coefficients, respectively. These virial coefficients are related to the coefficients A_{ij} and A_{ijk} used above (cf. Kurata, 1982):

$$A_2^{LS} = \frac{1}{M_w^2}\sum_{i=2}^{N}\sum_{j=2}^{N}\xi_i\xi_j M_i M_j A_{ij} \qquad (19)$$

$$A_3^{LS} = \frac{1}{M_w^2}\sum_{i=2}^{N}\sum_{j=2}^{N}\sum_{k=2}^{N}\xi_i\xi_j\xi_k M_i M_j A_{ijk} - $$

$$\frac{4}{3M_w^3}\sum_{i=2}^{N}\sum_{j=2}^{N}\sum_{k=2}^{N}\sum_{l=2}^{N}\xi_i\xi_j\xi_k\xi_l M_i M_j M_k M_l(A_{ij}A_{jk} - A_{ik}A_{jl}) \qquad (20)$$

It seems to be worth noticing explicitly some specific features of polydisperse polymers:

(1) For polydisperse polymers light-scattering virial coefficients A_2^{LS} and A_3^{LS} differ from *osmotic* virial coefficients A_2^{osm} and A_3^{osm}, whereas for monodisperse polymers there is no difference between *osmotic* and *light-scattering* virial coefficients $A_2^{osm} = A_2^{LS}$ and $A_3^{osm} = A_3^{LS}$.

(2) When the second virial coefficient A_{ij} depends on the molecular masses of fractions i and j, the light-scattering third virial coefficient A_3^{LS} depends also on second virial coefficients A_{ij}.

Pseudocomponents. The pseudocomponent approach was chosen for describing polydispersity. The molecular weight distribution of each dextran was approximated by a finite number of pseudocomponents. Various numbers of pseudocomponents (between 3 and 64) were tested for each dextran. For a fixed number of pseudocomponents, the molecular weight M_i and the weight fraction ξ_i of each pseudocomponent i were determined by applying an algorithm based on the Gaussian quadrature method (Stoer, 1979) using commercially available software (NAG): First, the molecular weights and the width of the intervals of pseudocomponents were determined by the Gaussian quadrature method; then the weight fractions of all pseudocomponents were determined with the restriction that the pseudocomponent approach gives the same weight-average molecular weight as that resulting from the molecular weight distribution function $f(M)$

$$\sum_{i=1}^{N}\xi_i M_i = \int_a^b f(M)M\,dM \qquad (21)$$

and also respecting the normalization

$$\sum_{i=1}^{N}\xi_i = \int_a^b f(M)\,dM = 1 \qquad (22)$$

N is the number of pseudocomponents, ξ_i is the weight fraction of each (monodisperse) pseudocomponent i in the polymer sample, M_i is the molecular weight of i, and $[a,b]$ is the interval of the molecular weight distribution.

Similar to results by Bogdanic and Fredenslund (1995) on VLE predictions of organic solvent−polymer systems, it was found that increasing the number of pseudocomponents beyond a certain limit has no influence on the calculated thermodynamic properties.

It proved to be sufficient to approximate the molecular weight distributions of dextran by eight pseudocomponents. As an example, the experimental results for the molecular weight distribution of DEX 110S and its approximation by eight pseudocomponents is shown in Figure 4. For all five
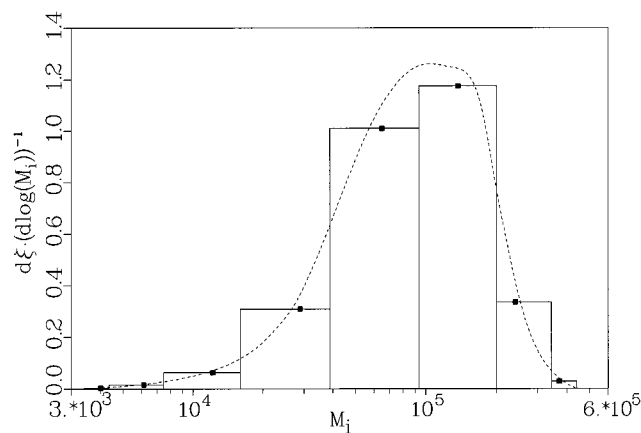

Figure 4. Approximation of the differential molecular weight distribution of DEX 110S by eight pseudocomponents.

dextrans the molecular weights of the pseudocomponents and their weight fractions are given in Table 9 in Appendix E.

Simultaneous Evaluation of Laser-Light-Scattering, Membrane Osmometric, and Isopiestic Data. Laser-light scattering and membrane osmometry are appropriate methods for determining the number- and weight-average molecular masses of polymers in low concentrated aqueous solutions. However, in order to get reliable information on second and third virial coefficients, additional experimental information at higher polymer concentrations is required. In the present work, experimental data from laser-light-scattering experiments, membrane osmometry (both at low concentrations), and isopiestic measurements (at high concentrations) were simultaneously evaluated.

For each monodisperse dextran, i.e., each pseudocomponent i ($i = 2, ..., N$) the virial coefficients A_{ii} and A_{iii} were expressed by two-parametric empirical expressions:

$$A_{ii} = \alpha_2 M_i^{\beta_2} \qquad (23)$$

$$A_{iii} = \alpha_3 M_i^{\beta_3} \qquad (24)$$

where α_j and β_j ($j = 2$ or 3) are constants. With these expressions, solutions of polydisperse polymers can be described either in the common way, i.e., assuming that virial coefficients depend on the molecular weight, or in the way described by Hasse et al. (1995) where virial coefficients are assumed to be independent of the molecular weight (i.e., $\beta_2 = \beta_3 = 0$).

The mixed virial coefficients A_{ij} and A_{ijk} were approximated using geometric mixing rules:

$$A_{ij} = (A_{ii}A_{jj})^{1/2} \qquad (25)$$

$$A_{ijk} = (A_{iii}A_{jjj}A_{kkk})^{1/3} \qquad (26)$$

For the simultaneous evaluation, the difference in temperature between the results from membrane osmometry (≈303 K) on one side and light scattering as well as isopiestic measurements (≈293 K) on the other side was neglected. This is no serious limitation as calorimetric investigations (Grossmann et al., 1995) proved that the influence of temperature on the excess Gibbs energy of aqueous solutions of dextran is very small in that temperature range.

The experimental results were evaluated for second and third osmotic virial coefficients of each aqueous dextran sample using two different methods. In method I it was

Table 4. Second (A_{22}) and Third (A_{222}) Virial Coefficients of Dextran in Aqueous Solution at around 293 K[a]

method I		method II
$\alpha_2/(10^{-3}\ \text{mol cm}^3\ \text{g}^{-2})$ $= 5.01$	$\beta_2 = -0.27$	$A_{22}/(10^{-4}\ \text{mol cm}^3\ \text{g}^{-2})$ $= 2.10$
$\alpha_3/(10^{-3}\ \text{mol cm}^6\ \text{g}^{-3})$ $= 5.21$	$\beta_3 = -0.025$	$A_{222}/(10^{-3}\ \text{mol cm}^6\ \text{g}^{-3})$ $= 4.22$

[a] Results of the simultaneous evaluation of experimental data using laser-light-scattering, membrane osmometry, and isopiestic experiments assuming that virial coefficients depend (method I: $A_{ii} = \alpha_2 M_i^{\beta_2}$, $A_{iii} = \alpha_3 M_i^{\beta_3}$) or do not depend (method II) on the molecular weight of the polymer.
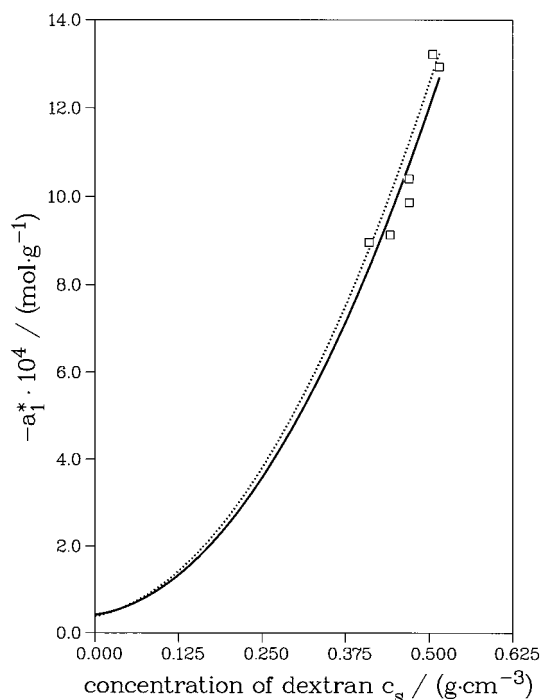

Figure 5. Reduced activity $a_1^* = \rho_1 \ln a_1(c_s)^{-1}$ of water in aqueous solutions of DEX 40VC at 293 K: □, experimental isopiestic measurements; ⋯ correlated method I; —, correlated method II.

assumed that the osmotic virial coefficients of dextran in water *depend* on the molecular weight of dextran (i.e., in eqs 23 and 24, $\beta_2 \neq 0$ and $\beta_3 \neq 0$), whereas in method II it was assumed that both osmotic virial coefficients *do not depend* on the polymer molecular weight (i.e., $\beta_2 = 0$ and $\beta_3 = 0$ in eqs 23 and 24). As has been described before (Hasse et al., 1995), in such an evaluation the number-average and the weight-average molecular weights of each dextran sample should not be taken from other experiments (like e.g. GPC) but have to be treated as adjustable parameters. However, for evaluating the results of the thermodynamic investigations by method I, the molecular weight distribution has to be known a priori. Therefore, in a first step, for evaluation by method I the results from the GPC measurements were only used to calculate weight fractions of the pseudocomponents. These weight fractions were used in eqs 10 and 11 and (together with the molecular weights of the pseudocomponents) in eqs 19 and 20. Then the remaining unknown parameters (i.e., number- and weight-average molecular weights M_n and M_w of each dextran sample and parameters α_2, α_3, β_2, β_3, and $\Lambda_{1,j}$ ($j =$ DEX 40S, DEX 40VC, DEX 70S, DEX 110S, DEX 500)) were fitted to the experimental results from the thermodynamic investigations by minimizing the objective func-
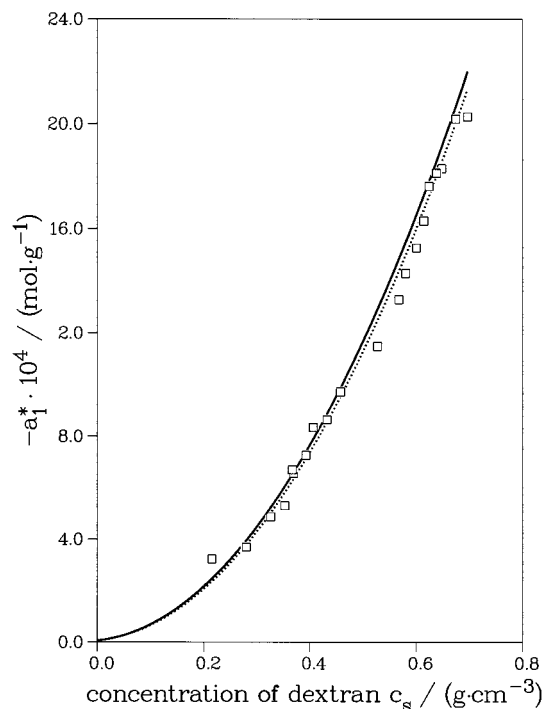

Figure 6. Reduced activity $a_1^* = \rho_1 \ln a_1(c_s)^{-1}$ of water in aqueous solutions of DEX 500 at 293 K: □, experimental isopiestic measurements; ⋯, correlated method I; —, correlated method II.

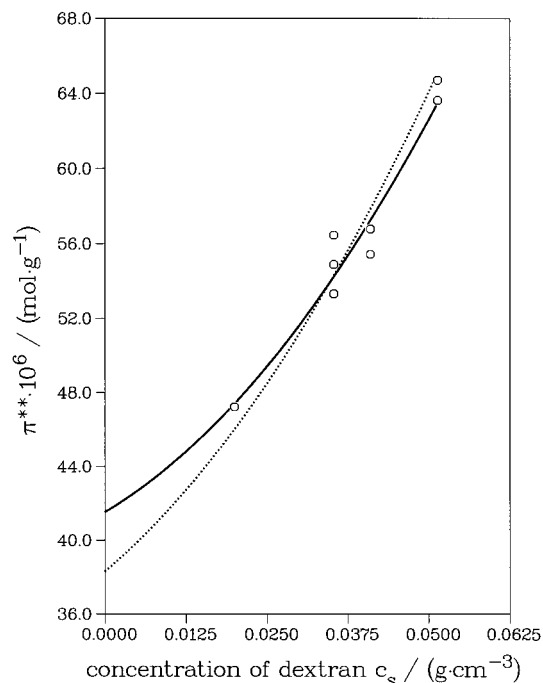**Figure 7.** Reduced osmotic pressure $\pi^{**} = \pi^*(RTc_s)^{-1}$ of aqueous solutions of DEX 40VC at 303 K: ○, experiment; ⋯, correlated method I; —, correlated method II.

tion SSQ:

$$SSQ = \frac{1}{N_{\text{LS}}}\sum_j^{N_{\text{LS}}}\left(\frac{Y_{\text{LS}j}^{\text{calc}} - Y_{\text{LS}j}^{\text{exp}}}{Y_{\text{LS}j}^{\text{exp}}}\right)^2 + \frac{1}{N_{\text{MO}}}\sum_j^{N_{\text{MO}}}\left(\frac{Y_{\text{MO}j}^{\text{calc}} - Y_{\text{MO}j}^{\text{exp}}}{Y_{\text{MO}j}^{\text{exp}}}\right)^2 + \frac{1}{N_{\text{ISO}}}\sum_j^{N_{\text{ISO}}}\left(\frac{Y_{\text{ISO}j}^{\text{calc}} - Y_{\text{ISO}j}^{\text{exp}}}{Y_{\text{ISO}j}^{\text{exp}}}\right)^2 \quad (27)$$

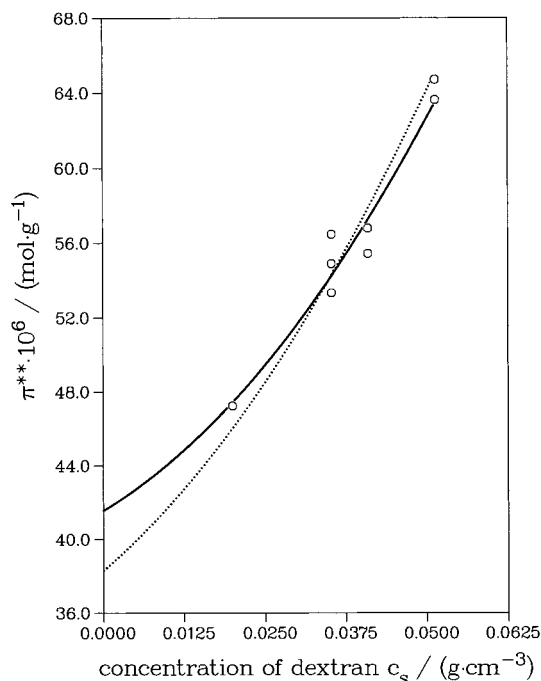The number-average molecular weights M_n and the weight-average molecular weights M_w of the samples

Figure 8. Reduced osmotic pressure $\pi^{**} = \pi^*(RTc_s)^{-1}$ of aqueous solutions of DEX 500 at 303 K: $\bigcirc$, experimental DEX 500; $\cdots$, correlated method I; $-$, correlated method II.
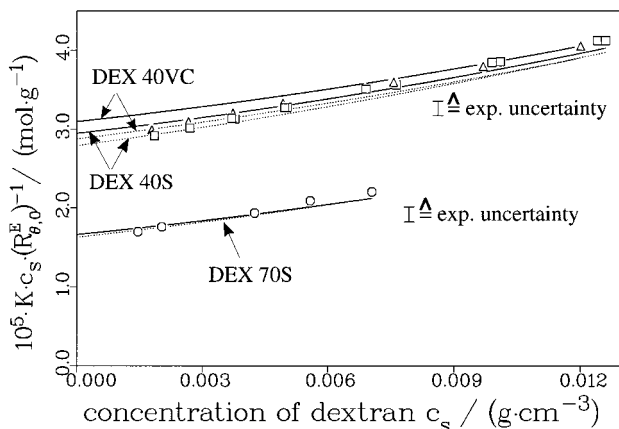

Figure 9. Laser-light-scattering data of aqueous solutions of DEX 40S, DEX 40VC, and DEX 70S at 293 K: $\square$, experimental DEX 40S; $\triangle$, experimental DEX 40S; $\bigcirc$, experimental DEX 70S; $\cdots$, correlated method I; $-$, correlated method II.

determined in that first evaluation of the thermodynamic data are not consistent with the GPC data. Therefore, a second evaluation was carried out after some adjustments in the molecular weight distribution from the GPC measurements. For that adjustment, the GPC results for the molecular weight distribution were first approximated by the sum of two Gauss−Lorentz functions:

$$\frac{d\xi}{d \log M_i} = GL_1 + GL_2 \tag{28}$$

GL_i stands for the Gauss−Lorentz function:

$$GL_i = \frac{a_i}{1 + b_i^2(M - c_i)^2} \exp(-d_i^2(M - c_i)^2) \tag{29}$$

For each dextran sample, parameters a_i, b_i, c_i, and d_i (i = 1, 2) were fitted to the GPC results for the molecular weight distribution. Then, two Gauss−Lorentz parameters
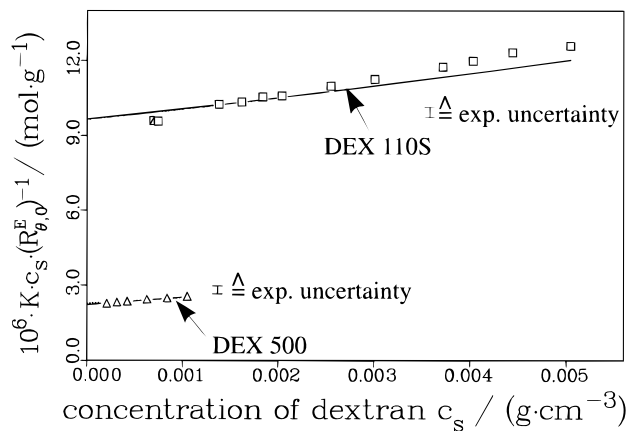

Figure 10. Laser-light-scattering data of aqueous solutions of DEX 110S and DEX 500 at 293 K: $\square$, experimental DEX 110S; $\triangle$, experimental DEX 500; $\cdots$, correlated method I; $-$, correlated method II (virtually the same curves for both methods).
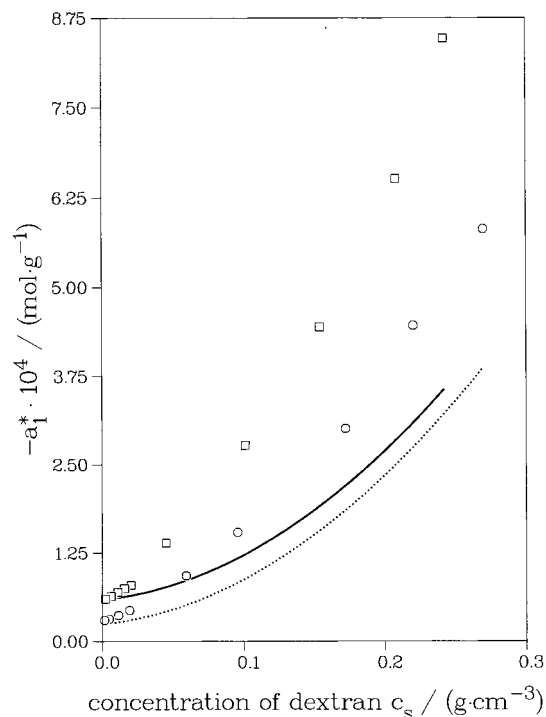

Figure 11. Reduced activity $a_1^* = \rho_1 \ln a_1(c_s)^{-1}$ of water in aqueous solutions of DEX 40 and 70 at 293 K. Comparison of experimental data by Gaube et al. (1993) with predictions: $\square$, experimental DEX 40; $\bigcirc$, experimental DEX 70; $-$, predicted DEX 40; $\cdots$, predicted DEX 70.

were adjusted to M_n and M_w from the "first step" evaluation of the experimental thermodynamic data. There is some arbitrariness in selecting those two parameters. However, the final results for the osmotic virial coefficients are not sensitive to that selection (Kany, 1998), and therefore no details are given here. The modified molecular weight distribution was again used to determine eight pseudocomponents and their weight fractions in each dextran sample. The evaluation was repeated several times to check its convergence for the adjusted molecular weight distribution. However, a single adjustment proved to be sufficient, as M_n and M_w determined in the evaluation of the thermodynamic properties in the "second step" already agreed very well with the results from the evaluation of the same data in the first step, and all further repetitions did not yield a significant change. Furthermore, also osmotic virial coef-
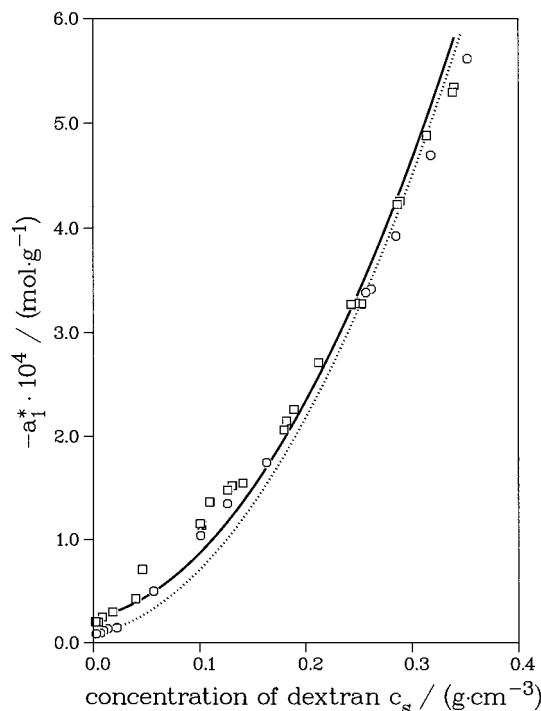
Figure 12. Reduced activity $a_1^* = \rho_1 \ln a_1(c_s)^{-1}$ of water in aqueous solutions of DEX 110 and 500 at 293 K. Comparison of experimental data by Gaube et al. (1993) with predictions: □, experimental DEX 110; ○, experimental DEX 500; —, predicted DEX 110; ···, predicted DEX 500.

Figure 13. Reduced activity $a_1^* = \rho_1 \ln a_1(c_s)^{-1}$ of water in aqueous solutions of DEX 70 and 500 at 293 K. Comparison of experimental data by Haynes et al. (1989) with predictions: □, experimental DEX 70; ○, experimental DEX 500; —, predicted DEX 70; ···, predicted DEX 500.

ficients calculated from the results of the first step evaluation with method I only slightly differed from those of the second step evaluation by the same method, and no significant change was observed when that second step evaluation was repeated.

In method II only parameters α_2, α_3, and $\Lambda_{1,j}$ (j = DEX 40S, DEX 40VC, DEX 70S, DEX 110S, DEX 500), of eqs 23, 24, and 18 were fitted to that objective function (cf. eq 27). For both methods (i.e., methods I and II), the final results for M_n and M_w of all dextran samples are given in Table 2 in comparison with the direct results from GPC measurements. The results for M_w from the GPC measurements of the present work agree well with the values provided by the suppliers. The maximum deviation is below 6% (for DEX 110S). However, the values for M_n and M_w from the results of the evaluation of the thermodynamic data—either from method I or II—are predominantly lower than the GPC results. The largest differences are observed for the low molecular dextran samples. It is assumed that this finding is due to difficulties in the detection of low molecular dextran fractions in GPC measurements. Both methods of evaluation (i.e., methods I and II) yield different values for the average molecular weights. For DEX 70S and DEX 110S the differences are below about 5%, whereas they increase to nearly 9% for lower molecular dextran (DEX 40S and DEX 40VC) and even 28% for higher molecular dextran (DEX 500). The results for the second and third osmotic virial coefficients of aqueous solutions of dextran at ambient temperature are given in Table 4. Additionally, the results for the second osmotic virial coefficient are also plotted in Figure 2. When no influence of the molecular weight on the osmotic virial coefficients of dextran in aqueous solution is assumed, the second osmotic virial coefficient is $A_{22}/(10^{-4} \text{ mol cm}^3 \text{ g}^{-2}) = 2.10$, while the evaluations assuming an influence of the molecular weight on the second osmotic virial coefficient result in $4.17 \geq A_{22}/(10^{-4} \text{ mol cm}^3 \text{ g}^{-2}) \geq 1.20$ for $10^4 \leq M_{\text{DEX}} \leq$
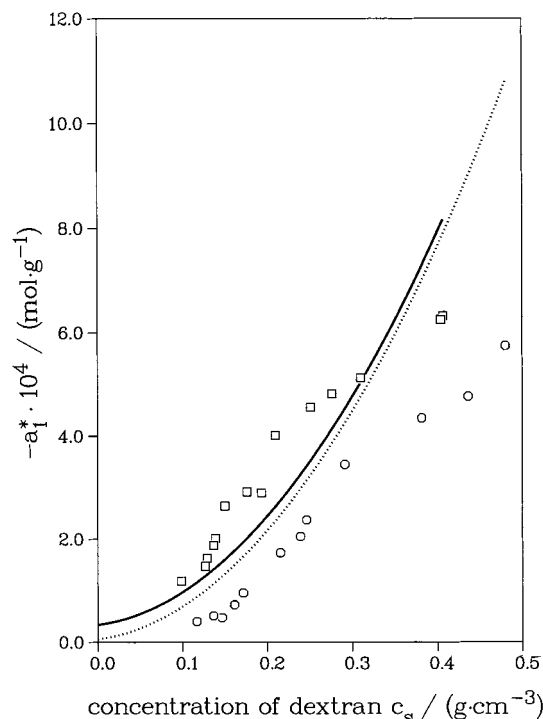

Figure 14. Reduced activity $a_1^* = \rho_1 \ln a_1(c_s)^{-1}$ of water in aqueous solutions of DEX 10 at 297 K. Comparison of experimental data by Jonsson (1984) with predictions: □, experimental DEX 10; —, predicted DEX 10.

10^6. Similarly, the result for the third osmotic virial coefficient of dextran in aqueous solution is $A_{222}/(10^{-3} \text{ mol cm}^6 \text{ g}^{-3}) = 4.22$ (assuming $A_{222} \neq f(M_{\text{DEX}})$) and $4.14 \geq A_{22}/(10^{-3} \text{ mol cm}^6 \text{ g}^{-3}) \geq 3.69$, for $10^4 \leq M_{\text{DEX}} \leq 10^6$ (assuming $A_{222} = f(M_{\text{DEX}})$). However, as is shown in the following chapter the results from both procedures (i.e., (A_{22}; A_{222}) $\neq f(M_{\text{DEX}})$ as well as (A_{22}; A_{222}) $= f(M_{\text{DEX}})$) are equally suited

Figure 15. Reduced activity $a_1^* = \rho_1 \ln a_1(c_s)^{-1}$ of water in aqueous solutions of DEX 130, 190, and 250 at 298 K. Comparison of experimental data by Mariani et al. (1955) with predictions: □, experimental DEX 130; —, predicted DEX 130; ○, experimental DEX 190; ···, predicted DEX 190; △, experimental DEX 250; - -, predicted DEX 250.
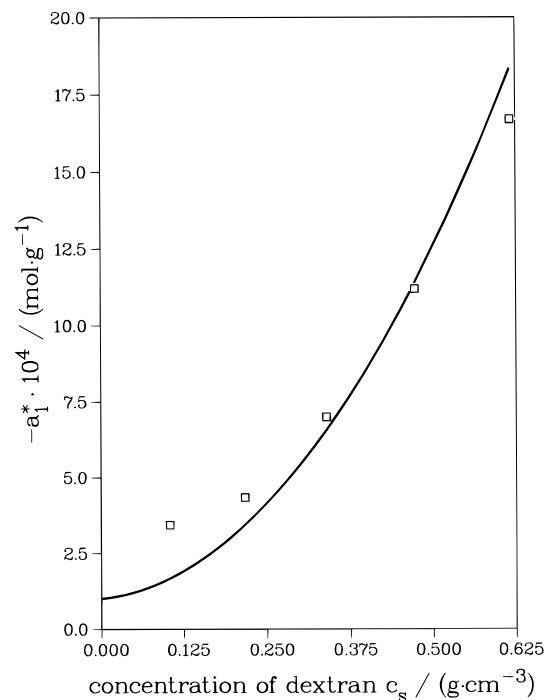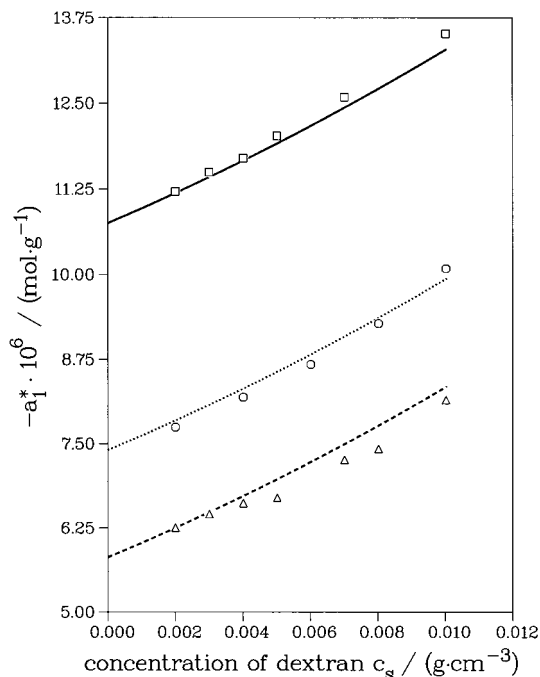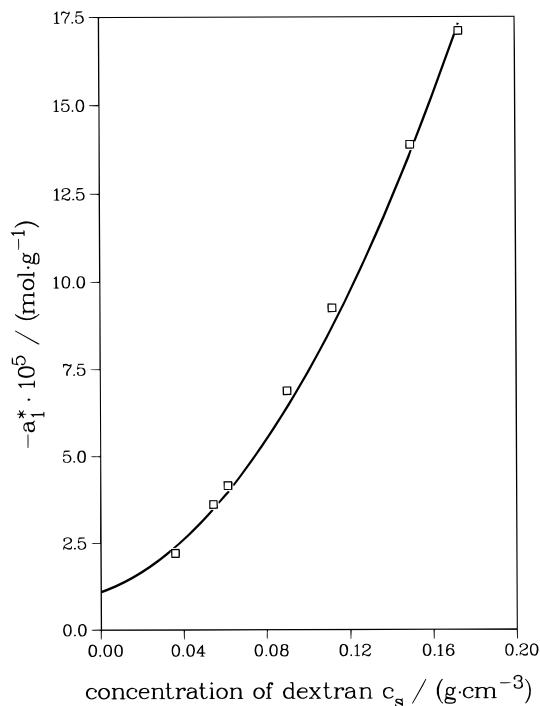

Figure 16. Reduced activity $a_1^* = \rho_1 \ln a_1(c_s)^{-1}$ of water in aqueous solutions of DEX 500 at 298 K. Comparison of experimental data by Vink (1971) with predictions: □, experimental DEX 500; —, predicted DEX 500.

to correlate the new experimental results from membrane osmometry, isopiestic measurements, and laser-light scattering.

Comparison of Correlated and New Experimental Data

As shown in Figure 5 (for DEX 40VC) and Figure 6 (for DEX 500), both methods are able to correlate the experi-
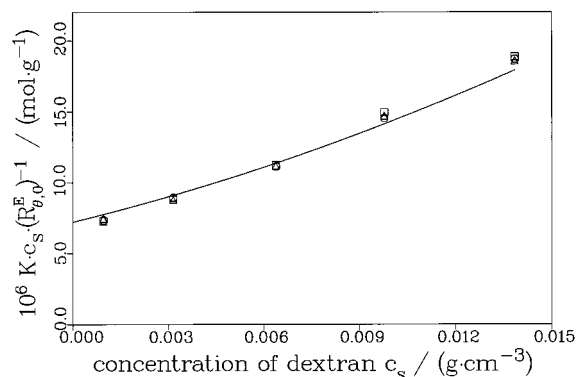

Figure 17. Laser-light-scattering data of aqueous solutions of DEX 158 at 280, 292, and 306 K. Comparison of experimental data by Comper and Laurent (1978) with predictions: □, experimental DEX 158, 280 K; ○, experimental DEX 158, 292 K; △, experimental DEX 158, 306 K; —, predicted.
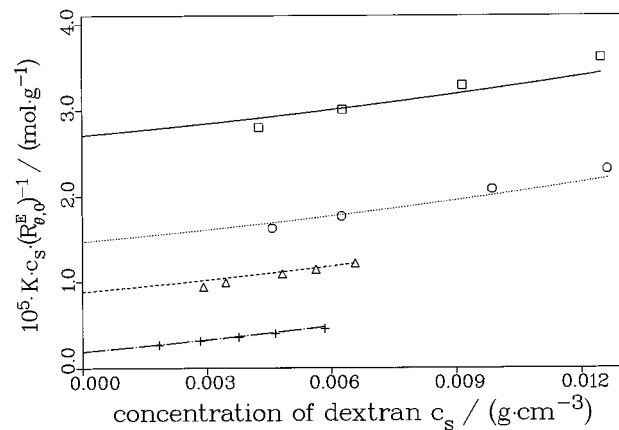
Figure 18. Laser-light-scattering data of aqueous solutions of DEX 40, DEX 70, DEX 110, and DEX 500 at 293 K. Comparison of experimental data by Stumpf (1993) with predictions: □, experimental DEX 40; ○, experimental DEX 70; △, experimental DEX 110; +, experimental DEX 500; —, predicted DEX 40; ···, predicted DEX 70; - -, predicted DEX 110; —·—, predicted DEX 500.

mental results for the activity of water from isopiestic measurements (i.e., at polymer concentrations between about 0.2 and 0.6 g cm⁻³) within the experimental uncertainty. A similar statement holds for the representation of the results at intermediate polymer concentrations (i.e., from about 0.025 to 0.07 g cm⁻³) determined by membrane osmometry (cf. Figures 7 and 8, for DEX 40VC and DEX 500, respectively). Also at very low polymer concentrations, both correlation methods give very similar results. This is demonstrated in Figures 9 and 10, where the averages of the extrapolated excess Rayleigh ratios (the experimentally determined excess Rayleigh ratios R_θ^E were extrapolated to $\theta = 0$ using eqs 17 and 18) are compared to the correlation for polymer concentrations between 0.0002 and 0.012 g cm⁻³.

Obviously, the new experimental data do not justify the assumption that the polymer molecular mass effects the second and third osmotic virial coefficient of aqueous solutions of dextran.

Comparison with Literature Data

In this section, literature data on thermodynamic properties of aqueous dextran solutions are compared with results from correlations from the present work. Thermodynamic properties of aqueous dextrans have been studied

Table 5. Specific Density of Aqueous Dextran Solutions

	$\rho^*/(\text{g cm}^{-3})$			$\rho^*/(\text{g cm}^{-3})$	
$\xi_s/(\text{g g}^{-1})$	293.15 K	313.15 K	$\xi_s/(\text{g g}^{-1})$	293.15 K	313.15 K
		DEX 40S			
0.0	0.9982	0.9922	0.0500	1.0182	1.0121
0.0062	1.0015	0.9956	0.1001	1.0391	1.0326
0.0100	1.0022	0.9961	0.1501	1.0608	1.0540
0.0121	1.0029	0.9975	0.1979	1.0822	1.0751
0.0200	1.0061	1.0001	0.3002	1.1310	1.1243
0.0242	1.0075	1.0015	0.3499	1.1544	1.1473
		DEX 40VC			
0.0065	1.0008	0.9950	0.0999	1.0391	1.0330
0.0124	1.0031	0.9971	0.2505	1.1067	1.0995
0.0249	1.0080	1.0020	0.3010	1.1307	1.1236
0.0501	1.0183	1.0120			
		DEX 70S			
0.0038	0.9998	0.9932	0.1003	1.0394	1.0327
0.0074	1.0010	0.9951	0.2496	1.1062	1.0991
0.0147	1.0039	0.9974	0.2992	1.1300	1.1229
0.0505	1.0186	1.0121			
		DEX 110S			
0.0023	0.9991	0.9933	0.0998	1.0390	1.0326
0.0044	0.9999	0.9941	0.2500	1.1062	1.0993
0.0089	1.0017	0.9956	0.3001	1.1303	1.1233
0.0491	1.0178	1.0117			
		DEX 500			
0.0010	0.9994	0.9934	0.1019	1.0404	1.0343
0.0030	0.9998	0.9937	0.1999	1.0840	1.0762
0.0102	1.0022	0.9959	0.3327	1.1468	1.1420
0.0470	1.0171	1.0130			

Table 6. Parameters of the Density Function for Aqueous Dextran Solutions

		DEX 40S, 40VC, 70S, 110S		DEX 500	
T/K	ρ_1^*	a	b	a	b
293	0.9982[a]	0.3943	0.1532	0.3949	0.1389
313	0.9922[a]	0.3886	0.1604	0.3886	0.1985

[a] Verein Deutscher Ingenieure, 1991.

by several authors using different methods, e.g., differential vapor-pressure measurements, vapor-pressure osmometry, membrane osmometry, laser-light scattering, and isopiestic investigations (cf. Table 1).

Second osmotic virial coefficients reported by different authors are compared to the results of the present work in Figure 2. That comparison reveals large differences. However, the reliability of the literature data is questionable mainly for two reasons. First, second virial coefficients were determined from measurements using a single experimental procedure in a rather limited concentration range, and, second, in the evaluation of the experimental data the polydispersity of the polymer as well as the third osmotic virial coefficients were neglected. Therefore, it is more reasonable to compare the direct experimental literature data (instead of a derived property) with the correlation of the present work.

In the frame of the present study, such comparison primarily aims at confirming/rejecting the assumption that the second virial coefficient of dextran in aqueous solution does not depend on the polymer molecular mass. Therefore, in the calculations it was assumed that $A_{22}/(10^{-4} \text{ mol cm}^3 \text{ g}^{-2}) = 2.10 \neq f(M_{\text{DEX}})$ and $A_{222}/(10^{-3} \text{ mol cm}^6 \text{ g}^{-3}) = 4.22 \neq f(M_{\text{DEX}})$. For the calculations, the molecular mass of the dextran samples was taken from the literature source of the experimental results, if not otherwise mentioned.

Gaube et al. (1993) report activities of water determined by membrane osmometry and vapor-pressure osmometry for four different dextrans (DEX 40, DEX 70, DEX 110, DEX 500). The experimental results for DEX 40 and DEX 70 show large deviations from the results of the present work (cf. Figure 11). The experimental data reveal a stronger influence of the concentration c_s on the reduced activity of water $a_1^* = \rho_1 \ln a_1(c_s)^{-1}$ than is predicted. However, the experimental data for DEX 110 and DEX 500 agree within the scattering of the data with the correlations of the present work (cf. Figure 12).

In Figure 13, the experimental results of Haynes et al. (1989) for the reduced activity of water are compared with the correlation of the present work. Haynes et al. determined the vapor pressure of aqueous solutions of DEX 70 and 500 by differential-vapor-pressure measurements. The experimental results of Haynes et al. show an unusual influence of the polymer concentration c_s ($0.1 \leq c_s/(\text{g cm}^{-3}) \leq 0.5$) on the reduced water activity a_1^*. Furthermore they reveal a large scattering. The predictions from the present work lie in between the scattering data.

Jonsson (1984) reports results from membrane osmometry for aqueous solutions of DEX 10. These results are compared to calculated data from the correlation of the present work in Figure 14. While, at intermediate and larger polymer concentrations, the predictions agree well with the experimental data, large deviations are observed at low concentrations. Obviously, the number given by Jonsson for the molecular mass of the studied dextran does not fit together with the experimental thermodynamic data.

Mariani et al. (1955) report activities of water determined by membrane osmometry for three different dextrans (DEX 130, DEX 190, DEX 250). The experimental data for all three dextrans agree very well with the correlations of the present work (cf. Figure 15).

Vink (1971) reports water activities measured by membrane osmometry of aqueous solutions of DEX 500. As the number for the averaged molecular mass of the dextran sample reported by Vink ($M_n/(\text{g mol}^{-1}) = 383\,430$) is obviously not in accordance with the reported experimental data, it was determined from the primary data of Vink, resulting in $M_n/(\text{g mol}^{-1}) = 91\,070$). Adapting that number results in a perfect agreement between experimental and predicted reduced activities of water (cf. Figure 16).

Comper and Laurent (1978) and Stumpf (1993) report laser-light-scattering data of aqueous solutions of dextran. The reported light-scattering data for three different temperatures between about 280 K and 306 K show no significant influence of the temperature on the excess Rayleigh ratios, i.e., the light scattering virial coefficients.

Table 7. Osmotic Pressure π^* in Aqueous Dextran Solutions at 303 K

DEX 40S		DEX 40VC		DEX 70S		DEX 110S		DEX 500	
$100\xi_s/(\text{g g}^{-1})$	π^*/Pa	$100\xi_s/(\text{g g}^{-1})$	π^*/Pa	$100\xi_s/(\text{g g}^{-1})$	π^*/Pa	$100\xi_s/(\text{g g}^{-1})$	π^*/Pa	$100\xi_s/(\text{g g}^{-1})$	π^*/Pa
1.772	1870^{+28}_{-21}	1.987	2399^{+36}_{-57}	1.999	1629^{+8}_{-8}	2.020	1243^{+76}_{-62}	2.510	941^{+36}_{-62}
2.961	3451^{+25}_{-33}	3.499	4855^{+99}_{-87}	3.035	2891^{+44}_{-70}	2.980	2166^{+89}_{-118}	4.573	2770^{+32}_{-56}
3.982	5695^a	4.049	584^{+68}_{-82}	5.005	6240^{+113}_{-87}	5.010	5229^{+208}_{-188}	6.582	6050^{+189}_{-209}
5.062	8370^{+135}_{-166}	5.056	8254^{+94}_{-93}						

[a] One data point.

Table 8. Experimental Results for the Activity of Water in Aqueous Solutions of DEX 40S, DEX 40VC, DEX 70S, and DEX 110S Determined by Isopiestic Measurements at 293 K

	polymer mass fraction (g g^{-1})			
a_1	DEX 40S	DEX 40VC	DEX 70S	DEX 110S
0.9948			0.3442	
0.9940			0.3560	
0.9937	0.3567			
0.9934		0.3546		0.3599
0.9932	0.3730			
0.9927		0.3779		0.3764
0.9917		0.3986		
0.9912			0.3867	
0.9912		0.3985		0.4069
0.9908	0.3842			
0.9899			0.4057	0.3985
0.9897			0.3970	0.3974
0.9896	0.4088		0.4068	
0.9881		0.4306		0.4371
0.9880		0.4236		0.4197
0.9878	0.4341			
0.9875			0.4163	0.4205
0.9868	0.4436			0.4468
0.9857			0.4581	
0.9849			0.4440	

This confirms that the influence of temperature on the activity coefficient of dextran in aqueous solutions can be neglected. The supplier's data for the molecular mass (M_w/(g mol^{-1}) = 158 000) reported by Comper and Laurent is not in accordance with the reported experimental data. A reevaluation of that data resulted in M_w/(g mol^{-1}) = 139 000. Using that number for M_w, the experimental results of Comper and Laurent for $Kc_s(R_{\theta,0}^E)^{-1}$ of low molecular dextran (DEX 10) in aqueous solution are well-predicted by the correlations of the present work (cf. Figure 17).

In Figure 18, the experimental results of Stumpf (1993) for aqueous solutions of dextran 40, 70, 110, and 500 solutions are compared with the correlation of the present work. As the molecular masses M_w reported by Stumpf were used, the calculations of the present work are predictions. Those predictions are in good agreement for all dextrans in the whole concentration range of the laser-light-scattering measurements.

Conclusions

Aqueous solutions of several dextran samples (DEX 40 to DEX 500) were investigated by laser-light-scattering, membrane osmometry, and isopiestic measurements at temperatures between 293 K and 303 K. The data cover a wide concentration range from very dilute to highly concentrated solutions. The results from different experiments were simultaneously evaluated to determine the second and third osmotic virial coefficients of dextran in aqueous solutions. The thermodynamic properties of aqueous dextran solutions can be accurately described by the osmotic

virial equation with virial coefficients which do not depend on the molecular mass of the dextran. The simple correlation presented here is successfully tested on literature data for dextran with weight-average molecular masses between 10 000 and 500 000 at concentrations up to 0.6 g cm^{-3}.

Appendix A: Densimetric Data

The specific density of aqueous solutions of DEX 40S, 40VC, 70S, 110S, and 500 was measured with a vibrating tube densimeter (Paar, Graz, Austria; type DMA 60) at 293 K and 313 K at polymer concentrations up to 0.35 g cm^{-3}. At each temperature, the densimeter was calibrated with bidistilled water and ethylene glycol (Riedel de Haen, Seelze, Germany; purity better than 0.995 g g^{-1}). The main experimental difficulty arises from the high viscosity of the solutions. The accuracy of the density data is estimated to be better than 2×10^{-4} g cm^{-3}. The accuracy of the temperature measurement is better than 0.5 K. It is found that, within the experimental uncertainty, there are no differences in the specific density of the aqueous solutions DEX 40S, 40VC, 70S, and 110S, whereas the density of DEX 500 is somewhat higher. The experimental results are given in Table 5. For each temperature the experimental data were correlated within their experimental uncertainty by

$$\rho^*/(\text{g cm}^{-3}) = \rho_1^* + a\xi_s + b\xi_s^2 \qquad (30)$$

Numbers for ρ_1^*, a, and b are given in Table 6.

Appendix B: Results from Membrane Osmometry

The results of membrane osmometric experiments are given in Table 7.

Appendix C: Results from Isopiestic Measurements

The results of isopiestic measurements are given in Table 8.

Appendix D: Particle Scattering Function

Debye (1915) derived a Taylor series expansion for P_θ:

$$P_\theta = 1 - \Lambda_0 \sin^2(\theta/2) + \Lambda_1 \sin^4(\theta/2) - ... \qquad (31)$$

where Λ_i are coefficients of the Taylor series. The first coefficient depends on the size of a polymer molecule (see, for example, Kurata (1982)):

$$\Lambda_0 = \frac{16\pi^2}{3\lambda^2}\langle S^2 \rangle \qquad (32)$$

$\langle S^2 \rangle^{0.5}$ is the mean-square radius of gyration of a polymer molecule. $\langle S^2 \rangle^{0.5}$ is related to the mean-square radii of gyration $\langle S^2 \rangle_i^{0.5}$ of the pseudocomponents i of each polymer

Table 9. Pseudocomponents for DEX Samples

DEX 40S		DEX 40VC		DEX 70S		DEX 110S		DEX 500	
M_i/(g mol^{-1})	ξ_i/(g g^{-1})	M_i/(g mol^{-1})	ξ_i/(g g^{-1})	M_i/(g mol^{-1})	ξ_i/(g g^{-1})	M_i/(g mol^{-1})	ξ_i/(g g^{-1})	M_i/(g mol^{-1})	ξ_i/(g g^{-1})
2 788	0.000 54	3 310	0.000 76	6 208	0.000 47	4 007	0.000 42	12 328	0.000 49
4 150	0.000 03	4 864	0.000 48	8 651	0.001 75	6 136	0.003 71	22 299	0.005 75
8 062	0.008 98	9 517	0.032 84	15 292	0.009 96	12 155	0.020 91	45 104	0.017 84
17 558	0.175 7	19 979	0.326 5	30 023	0.125 7	28 897	0.119 1	108 125	0.088 1
33 630	0.540 1	38 568	0.480 4	54 194	0.495 2	65 140	0.386 3	257 849	0.336 0
65 327	0.232 1	77 246	0.140 8	94 655	0.322 6	137 635	0.388 4	534 104	0.395 8
115 698	0.038 44	137 104	0.013 62	149 051	0.043 18	240 882	0.077 99	1 009 226	0.131 0
171 539	0.002 54	206 709	0.000 37	213 958	0.001 13	370 559	0.003 14	1 551 900	0.025 44

by (cf. Kurata (1982))

$$\langle S^2 \rangle = \frac{1}{M_w} \sum_{i=2}^{N} \xi_i M_i \langle S^2 \rangle_i^{0.5} \tag{33}$$

It was assumed that Λ_1 is an adjustable parameter characterizing each polydisperse polymer sample (i.e., $\Lambda_{1,\text{DEX40S}} \neq \Lambda_{1,\text{DEX40VC}} \neq ...$). In preliminary calculations the mean-square radius of gyration $\langle S^2 \rangle_i^{0.5}$ of each pseudocomponent i was approximated by

$$\langle S^2 \rangle_i^{0.5} = \gamma M_i^{\delta} \tag{34}$$

and parameters γ, δ were also fitted to the experimental results (together with all other parameters) by optimizing the objective function given in eq 27. However, the results for Λ_0 were so small that within the experimental uncertainty the contribution of $\Lambda_0 \sin^2(\theta/2)$ to P_θ in eq 31 can be neglected. Therefore the final evaluation was performed with the approximation

$$P_\theta = 1 + \Lambda_1 \sin^4(\theta/2) \tag{35}$$

Parameters Λ_1 are given in Table 3.

Appendix E: Pseudocomponents

The molecular mass distribution of the dextran samples was determined by gel permeation chromatography and approximated by introducing eight pseudocomponents. Information on that approximation (molecular mass and mass fraction of each pseudocomponent) is given in Table 9.

Nomenclature

A	osmotic virial coefficient
a	activity
a^*	reduced activity, $a_1^* = \rho_1 \ln a_1(c_s)^{-1}$
a	constant related to the osmotic virial coefficient by eqs 13 and 14
a	lower bound of an interval
a	parameter of a Gauss–Lorentz function
b	upper bound of an interval
b	parameter of a Gauss–Lorentz function
c	concentration in mass/volume
c	parameter of a Gauss–Lorentz function
corr	correlated
DEX	dextran
d	parameter of a Gauss–Lorentz function
exp	experimental
$f(M)$	molecular mass distribution function
G	Gibbs energy
GL	Gauss–Lorentz function
GPC	gel permeation chromatography
K	optical constant
ISO	isopiestic method
M	molecular weight
MALLS	multiangle laser-light scattering
MO	membrane osmometry
m	mass
N	number of data points
N	number of pseudocomponents
N_A	Avogadro's number
n	number of moles
n	refractive index of the solution (function of T and c)
na	not available
P	particle scattering function
PEG	poly(ethylene glycol)
p	pressure
R	universal gas constant
R	Rayleigh ratio
S	radius of gyration
SSQ	objective function (weighted sum of squares)
T	temperature
V	volume
w	weight
Y	measured quantity

Greek Symbols

α	parameter
β	parameter
γ	parameter
γ	activity coefficient (function of T and c)
δ	parameter
Λ	parameter of particle scattering function
λ	laser wavelength
π^*	osmotic pressure
π^{**}	reduced osmotic pressure, $\pi^{**} = \pi^*(RTc_s)^{-1}$
θ	angle
ξ	mass fraction
ρ	molar density
ρ^*	specific density

Subscripts

0	zero angle
1	solvent (water); also, pure solvent at T_{mix}
2	second osmotic virial coefficient
3	third osmotic virial coefficient
i	component i
ij	binary virial coefficient of components i and j
ijk	ternary virial coefficient of components i, j, and k
ISO	isopiestic method
j	component j
k	component k
LS	light scattering
MO	membrane osmometry
n	number average
s	solute (i.e., DEX)
w	weight average
θ	angle

Superscripts

calc	calculated
E	excess
osm	osmotic virial coefficient
LS	light-scattering virial coefficient

Literature Cited

Albertsson, P. *Partition of Cell Particles and Macromolecules*, 3rd ed.; John Wiley & Sons: New York, 1986.

Basedow, A. M.; Ebert, K. H.; Feigenbutz, W. Polymer-Solvent Interactions: Dextran in Water and DMSO. *Makromol. Chem.* **1980**, *181*, 1071–1080.

Bogdanic, G.; Fredenslund, A. Prediction of Vapor–Liquid Equilibria for Mixtures with Copolymers. *Ind. Eng. Chem.* **1995**, *34*, 324–331.

Burchard, W.; Pfannenmüller, B. Molekulargewichte von Dextran und Dextrantricarbanilat des Bakterienstammes Leuconostoc mesenteroides B 512. *Makromol. Chem.* **1969**, *121*, 18–32.

Cesi, V.; Katzbauer, B.; Narodoslawsky, M. In *Thermophysical Properties of Polymers in Aqueous Two-Phase Systems*, Presentation; Moser, A., Ed.; 12th Symposium on Thermophysical Properties; Boulder, Colorado, 1994.

Comper, W. D.; Laurent, T. C. An Estimate of the Enthalpic Contribution to the Interaction between Dextran and Albumin. *Biochem. J.* **1978**, *175*, 703–708.

Debye, P. Zerstreuung von Röntgenstrahlen. *Ann. Phys.* **1915**, *46*, 809.

Edmond, E.; Ogston, A. G. An Approch to the Study of Phase Separation in Ternary Aqueous Systems. *Biochem. J.* **1968**, *109*, 569–576.

Edsman, K.; Sundelöf, L.-O. Interaction virial coefficients in some mixed polymer solutions. *Polymer* **1988**, *29*, 535–540.

Fedin, E. I.; Tsitsishvili, V. G.; Grindberg, V. Y.; Bakari, T. I.; Tolstoguzov, V. B. A Study of Dextran Hydration in Dilute, Aqueous Solution by the Proton Magnetic Relaxation Method. *Carbohydr. Res.* **1975**, *39*, 193–199.

Gaube, J.; Pfennig, A.; Stumpf, M. Vapor–Liquid Equilibrium in Binary and Ternary Aqueous Solutions of Poly(ethylene glycol) and Dextran. *J. Chem. Eng. Data* **1993**, *38*, 163–166.

Gekko, K. Physiochemical Studies of Oligodextran (III) Thermodynamic Studies of Dextran Aqueous Solution by Vapor Pressure Lowering Method. *J. Sci. Hiroshima Univ.* **1971**, *35* (2), 111–121.

Gekko, K.; Noguchi, H. Physicochemical Studies of Oligodextran. I. Molecular Weight Dependence of Intrinsic Viscosity, Partial Specific Compressibility and Hydrated Water. *Biopolymers* **1971**, *10*, 1513–1524.

Granath, K. A. Solution Properties of Branched Dextran. *J. Colloid Sci.* **1958**, *13*, 308–328.

Granger, H. J.; Laine, S. H.; Laine, G. A. Osmotic Pressure Experted by Entangled Polysaccharide Chains. *Microcirc., Endothelium, Lymphatics* **1985**, *2*, 85–105.

Grossmann, C.; Tintinger, R.; Zhu, J.; Maurer, G. Aqueous Two-Phase Systems of Poly(ethylene glycol) and Dextran-Experimental Results and Modeling of Thermodynamic Properties. *Fluid Phase Equilib.* **1995**, *106*, 111–138.

Hasse, H.; Kany, H.-P.; Tintinger, R.; Maurer, G. Osmotic Virial Coefficients of Aqueous Poly(ethylene Glycol) from Laser-Light Scattering and Isopiestic Measurements. *Macromolecules* **1995**, *28*, 3540–3552.

Haynes, C. A.; Beynon, R. A.; King, R. S.; Blanch, H. W.; Prausnitz, J. M. Thermodynamic Properties of Aqueous Polymer Solutions: Poly-(ethylene glycol)/Dextran. *J. Phys. Chem.* **1989**, *93*, 5612–5617.

Jackson, C.; Nilsson, L. M.; Wyatt, P. J. Characterization of Biopolymers using a Multi-Angle Light Scattering Detector with Size Exclusion Chromatography. *J. Appl. Polym. Sci.* **1989**, *43* (99), 99–114.

Jeremić, K.; Ilić, L.; Lechner, M. D.; Jovanović, S. The influence of temperature on dextran behaviour in dilute aqueous solutions. *J. Serb. Chem. Soc.* **1992**, *57* (9), 571–577.

Johansson, G.; Joelsson, M. Some Physical Measurements in the One-Phase Region of a Water-Dextran-Poly(ethylene glycol) System. *Polymer* **1992**, *33* (1), 152–155.

Jonsson, G. Boundary Layer Phenomena During Ultrafiltration of Dextran and Whey Protein Solutions. *Desalination* **1984**, *51*, 61–77.

Kany, H.-P. Thermodynamische Eigenschaften Wässriger Polymerlösungen. Ph.D. Thesis, Universität Kaiserslautern, Kaiserslautern, 1998.

King, R. S.; Blanch, H. W.; Prausnitz, J. M. Molecular Thermodynamics of Aqueous Two-Phase Systems for Bioseparations. *AIChE J.* **1988**, *34* (10), 1585–1594.

Kirkwood, J. G.; Goldberg, R. J. Light Scattering Arising from Composition Fluctuations in Multi-Component Systems. *J. Chem. Phys.* **1950**, *18* (1), 54–57.

Kratochvíl, P. *Classical Light Scattering from Polymer Solutions*; Elsevier: Amsterdam, 1987.

Kurata, M. *Thermodynamics of Polymer Solutions*; Harwood Academic Publishers: Chur, Switzerland, 1982.

Mariani, E.; Ciferri, A.; Maraghini, M. Osmotic Measurements on Dilute Dextran Solutions. *J. Phys. Chem.* **1955**, *18*, 303–304.

Nordmeier, E. Static and Dynamic Light-Scattering Solution Behavior of Pullulan and Dextran in Comparison. *J. Phys. Chem.* **1993a**, *97*, 5770–5785.

Nordmeier, E. Static and dynamic light scattering studies of dextran from Leuconostoc Mesenteroides in the dilute region. *Makromol. Chem.* **1993b**, *194*, 2923–2937.

Numerical Algorithms Group. *NAG Fortran Library Manual*; Numerical Algorithms Group: Oxford, U.K., 1989.

Pusch, W. Osmotic Pressure of Dextran T10 Solutions. *Desalination* **1988**, *68*, 69–73.

Rathbone, S. J.; Haynes, C. A.; Blanch, H. W.; Prausnitz, J. M. Thermodynamic Properties of Dilute Aqueous Polymer Solutions from Low-Angle Laser-Light-Scattering Measurements. *Macromolecules* **1990**, *23*, 3944–3947.

Riddick, J. A.; Bunger, W. B.; Sakano, T. K. *Organic Solvents: Physical Properties and Methods of Purification*, 4th ed.; John Wiley & Sons: New York, 1986; Vol. II.

Senti, F. R.; Hellman, N. N.; Ludwig, N. H.; Babcock, G. E.; Tobin, R.; Glass, C. A.; Lamberts, B. L. Viscosity, Sedimentation, and Light-Scattering Properties of Fractions of an Acid-Hydrolyzed Dextran. *J. Polym. Sci.* **1955**, *17*, 527–546.

Smit, J. A.; Dijk, J. A. P.; Mennen, M. G.; Daoud, M. Polymer Size Exponents of Branched Dextrans. *Macromolecules* **1992**, *25*, 3585–3590.

Stockmayer, W. H. Light Scattering in Multi-Component Systems. *J. Chem. Phys.* **1949**, *18* (1), 58–61.

Stoer, J. *Einführung in die Numerische Mathematik I*; Springer-Verlag: Heidelberg, New York, 1979.

Stumpf, M. Thermodynamische Untersuchungen zu wässrigen PEG-Dextran-Zweiphasensystemen und Bestimmung des Salzeinflusses auf das Phasenverhalten. Ph.D. Thesis, Technische Hochschule, Darmstadt, Germany, 1993.

Verein Deutscher Ingenieure. *VDI-Wärmeatlas*, 6th ed.; VDI-Gesellschaft Verfahrenstechnik und Chemieingenieurwesen (GVC), Ed.; VDI-Verlag GmbH: Düsseldorf, Germany, 1991.

Vink, H. Precision Measurements of Osmotic Pressure in Concentrated Polymer Solutions. *Eur. Polym. J.* **1971**, *13*, 1411–1419.

Williams, D. L.; Pretus, H. A.; Browder, I. W. Application of Aqueous Gel Permeation Chromatography with In-Line Multi-Angle Laser Light Scattering and Differential Viscosimetry Detectors for the Characterization of Natural Product Carbohydrate Pharmaceuticals. *J. Liq. Chromatogr.* **1992**, *14* (13), 2297–2309.